A tsunami forecast model for Cordova, Alaska

Chris Chamberlin

NOAA Center for Tsunami Research
Pacific Marine Environmental Laboratory

September 2011

DRAFT

Figures

Figure 1 [cordova-locator]. Location of Cordova, Alaska, and other nearby planned and existing tsunami forecast model sites.

Figure 2 [cordova-pws-locator]. Topographic relief of Prince William Sound.

Figure 3 [cordova-orcainlet]. Summary of Orca Inlet bathymetry, showing the extensive shoals that dry at low tide. Circled red dot indicates Cordova tide gauge location.

Figure 4 [grid-extents]. Modeling grid extents. red forecast model blue reference model. dashed contour 200m, solid contours 1000 m interval.

Figure 5 [cordova-detail-profiles]. Detail of Cordova, Alaska, from NOS chart #16710. Shaded elevation from 1 arc-second resolution grid developed by NGDC (Grothe et al 2010).

Figure 6 [profile-graph]. Across-shoreline elevation profiles in the Cordova area. Fig. [cordova-detail-profiles] shows the profile locations.

Figure 7 [ak1964-wilson]. Estimated tsunami wave amplitudes at Cordova, Alaska during the March 28, 1964 tsunami, inferred from eyewitness reports. Reproduced from Wilson and Tørum (1974) p. 472.

Figure 8 [unimak1946]. Modeled wave amplitudes for the 1 April 1946 Unimak tsunami. a) Maximum amplitude for reference model, b) Maximum amplitudes for forecast model, c) timeseries at tide gauge point with reference model in blue and forecast model in red.

Figure 9 [andreanof1957]. Modeled wave amplitudes for the 9 March 1957 Andreanov Islands tsunami. a) Maximum amplitude for reference model, b) Maximum amplitudes for forecast model, c) timeseries at tide gauge point with reference model in blue and forecast model in red.

Figure 10 [alaska1964]. Modeled wave amplitudes for the 28 March 1964 Alaska tsunami. a) Maximum amplitude for reference model, b) Maximum amplitudes for forecast model, c) timeseries at tide gauge point with reference model in blue and forecast model in red.

Figure 11 [kuril1994]. Modeled wave amplitudes for the 4 October 1994 Kuril Islands tsunami. a) Maximum amplitude for reference model, b) Maximum amplitudes for forecast model, c) timeseries at tide gauge point with reference model in blue and forecast model in red.

Figure 12 [solomon2007]. Modeled wave amplitudes for the 1 April 2007 Solomon Islands tsunami. a) Maximum amplitude for reference model, b) Maximum amplitudes for forecast model, c) timeseries at tide gauge point with reference model in blue and forecast model in red.

Figure 13 [chile20100227]. Modeled and recorded wave amplitudes for the 27 February 2010 Chile tsunami. a) Maximum amplitude for reference model, b) Maximum amplitudes for forecast model, c) timeseries at tide gauge point with reference model in blue, forecast model in red, and de-tided tide gauge signal in black.

Figure 14 [japan2011]. Modeled and recorded wave amplitudes for the 27 February 2010 Chile tsunami. a) Maximum amplitude for reference model, b) Maximum amplitudes for forecast model, c) timeseries at tide gauge point with reference model in blue, forecast model in red, and de-tided tide gauge signal in black.

Figure 15 [stability-all]. Results of stability testing using twenty Mw 9.3 scenarios located along all Pacific Ocean subduction zones. Reference model in blue, forecast model in red.

Introduction

The National Oceanic and Atmospheric Administration (NOAA) Center for Tsunami Research (NCTR) at the NOAA Pacific Marine Environmental Laboratory (PMEL) has developed a tsunami forecasting system for operational use by NOAA's two Tsunami Warning Centers located in Hawaii and Alaska (Titov et al., 2005). The system is designed to efficiently provide basin-wide warning of approaching tsunami waves accurately and quickly. The system, termed Short-term Inundation Forecast of Tsunamis (SIFT), combines real-time tsunami event data with numerical models to produce estimates of tsunami wave arrival times and amplitudes at a coastal community of interest. The SIFT system integrates several key components: deep-ocean observations of tsunamis in real time, a basin-wide pre-computed propagation database of water level and flow velocities based on potential seismic unit sources, an inversion algorithm to refine the tsunami source based on deep-ocean observations during an event, and high-resolution tsunami inundation forecast models.

This report documents the development of a tsunami inundation forecast model covering the community of Cordova, Alaska. This operational forecast model is designed for integration into the SIFT system.

Forecast Methodology

A high-resolution inundation model was used as the basis for development of a tsunami forecast model to operationally provide an estimate of wave arrival time, wave height, and inundation at Cordova following tsunami generation. All tsunami forecast models are run in real time while a tsunami is propagating across the open ocean. The model was designed and tested to perform under stringent time constraints given that time is generally the single limiting factor in saving lives and property. The goal of this work is to maximize the length of time that the community of Cordova has to react to a tsunami threat by providing accurate information quickly to emergency managers and other officials responsible for the community and infrastructure.

The general tsunami forecast model, based on the Method of Splitting Tsunami (MOST), is used in the tsunami inundation and forecasting system to provide real-time tsunami forecasts at selected coastal communities. The model runs in minutes while employing high-resolution grids constructed by the National Geophysical Data Center. MOST is a suite of numerical simulation codes capable of simulating three processes of tsunami evolution: earthquake, transoceanic propagation, and inundation of dry land. The model has been extensively tested against a number of laboratory experiments and benchmarks (Synolakis et al. 2008) and was successfully used for simulations of many historical tsunami events. The main objective of a forecast model is to provide an accurate, yet rapid, estimate of wave arrival time, wave height, and inundation in the minutes following a tsunami event. Titov and González (1997) describe the technical aspects of inundation model development, stability, testing, and robustness, and Tang et al. (2009) provide detailed forecast methodology.

A basin-wide database of pre-computed water elevations and flow velocities for unit sources covering worldwide subduction zones has been generated to expedite forecasts (Gica et al. 2008). As the tsunami wave propagates across the ocean and successively

reaches tsunameter observation sites, recorded sea level is ingested into the tsunami forecast application in near real-time and incorporated into an inversion algorithm to produce an improved estimate of the tsunami source. A linear combination of the pre-computed database is then performed based on this tsunami source, now reflecting the transfer of energy to the fluid body, to produce synthetic boundary conditions of water elevation and flow velocities to initiate the forecast model computation.
Accurate forecasting of the tsunami impact on a coastal community largely relies on the accuracies of bathymetry and topography and the numerical computation. The high spatial and temporal grid resolution necessary for modeling accuracy poses a challenge in the run-time requirement for real-time forecasts. Each forecast model consists of three telescoped grids with increasing spatial resolution in the finest grid, and temporal resolution for simulation of wave inundation onto dry land. The forecast model utilizes the most recent bathymetry and topography available to reproduce the correct wave dynamics during the inundation computation. Forecast models, including the Cordova model, are constructed for at-risk coastal communities in the Pacific and Atlantic Oceans. Previous and present development of forecast models in the Pacific (Titov et al. 2005; Tang et al. 2008; Wei et al. 2008; Titov 2009) have validated the accuracy and efficiency of each forecast model currently implemented in the real-time tsunami forecast system.

Model setting

Cordova, Alaska is a town of 2,240 people (2009 estimate) located on Orca Inlet in eastern Prince William Sound, central Alaska. The town was founded in 1906 as a railroad terminal and shipping port to serve copper, gold, and silver mines located in the Copper River delta. The mines and railroad closed in 1938, and economic activity in the town is now dominated by commercial fishing. Salmon is the most prominent fishery in Cordova, with over 360 commercial salmon fishing permits issued in the town in 2000; other major fisheries are halibut and herring. As of 2000, the town was home to eight fish processing plants, as well as a large marina facility. The town also has a substantial sport fishing industry (Sepez et al 2005). Most land near Cordova is managed by the Chugach National Forest (United States Forest Service) or by the Eyak Corporation, an Alaska native corporation.

Transportation to Cordova from the rest of Alaska is by air or water only; there is no road connection the highway system. Local roads run northeast and southwest from the town center; a cannery is located at the end of the northeastern road in the village of Orca. The town is served by commercial airlines and by the state-owned Alaska Marine Highway ferry system.

Cordova is the northernmost tsunami forecast model currently planned for development (Fig. [cordova-locator]), and the only model in Prince William Sound. The town is located on the west shore of Orca Inlet in the far eastern part of Prince William Sound, and just west of the Copper River delta (Fig. [cordova-pws-locator]). It is well-protected from the open Pacific Ocean. While Orca Inlet to the south of the town opens into the Pacific Ocean, most of the inlet is shoal; extensive areas dry at low tide, leaving only narrow channels (Fig. [cordova-orcainlet]). As is described later, this extensive

shoal area effectively protects Cordova from most tsunami wave energy approaching from the open ocean. The closest deep-water passage to Cordova is via 12-km-wide Hinchinbrook Entrance, Prince William Sound's major entrance, 60 km west of the town. From the entrance, the route to Cordova passes east through deep Orca Bay, then through narrow (1 km wide) channels to the north of town (Coast Pilot 2011).

Prince WIlliam Sound has semidiurnal tides with a substantial tide range; at Cordova, the mean tidal range is 3.10 m. The tidal flood current at Cordova enters Orca Inlet from the northeast, and flows southwest past the Cordova waterfront; flood tide velocities reach 0.9 m/s (1.8 knots), and ebb tides are 0.5 m/s (1 knot) (Coast Pilot 2011).

NOAA's National Ocean Service has operated a tide gauge (station ID 9454050) at Cordova since May 1949. The tide station is located approximately 1 km north of the town center on the southern end of the public ferry dock, at (60.5575°N, 145.7554°W). Water depth at the tide station, according to the source bathymetry grid (Grothe et al 2010), is approximately 9 m below mean high water.

Historical tsunami record

The March 28, 1964 Prince William Sound earthquake (Mw=9.2) is the only recorded historical earthquake to have caused damage in Cordova (Lander 1996). Located within the great earthquake's rupture zone, the town was subject to coseismic vertical uplift of approximately 2 m. There is no surviving tide gauge record from the event, but Wilson and Tørum (1972) developed an "inferred marigram" from reports of witnesses on the site; this is reproduced in Figure [ak1964-wilson]. It shows the first major wave arriving at Cordova 1 hour 25 minutes after the earthquake, the largest drawdown (8.2 m below original MLLW) 2h 45m after the event. The highest wave, 6 hours after the event, was estimated at 9.8 m above original MLLW. As the diagram indicates, the initial tsunami waves arrived near low astronomical tide, so the highest waves relative to MLLW arrived much later, near high tide. The highest runup recorded was 4.2 m (Lander 1996) above the predicted astronomical tide level. The tsunami caused substantial damage to waterfront structures, and maximum horizontal inundation extent may have reached 90 m.

Because of Cordova's well-protected location, other historical trans-Pacific tsunamis have not produced substantial waves at the town. There is no record of the May 22, 1960 Chile earthquake at Cordova, but nearby Valdez (northeastern Prince William Sound) reportedly had no noticeable tsunami signal (Lander 1996). The two major Pacific-basin tsunamis to occur since the 1964 event, the February 2, 2010 Chile (Mw 8.8) and March 11, 2011 (Mw 9.0) Japan tsunamis, produced 13 cm and 9 cm runups at Cordova, respectively. For both of these events, the recording at Cordova was among the smallest in Alaska (National Geophysical Data Center/World Data Center Historical Tsunami Database).

Topographic and bathymetric data

The model grids were derived from a set of combined bathymetric/topographic grids developed by NOAA's National Geophysical Data Center. Three source grids were

used: two high-resolution grids covering the Cordova area at 3 arc-second and 1/3 arc-seconds resolutions (Grothe *et al* 2010) and one medium-resolution grid covering all of Prince William Sound at 8 arc-seconds (Caldwell et al 2009). The highest-resolution 1/3 arc-second (≈10 m) grid covers the deep-water Orca Bay approach to Cordova and the Cordova harbor area. Because of a lack of high-resolution survey data in the shallow Orca Inlet and Copper River Delta areas, these are covered at 3 arc-seconds (≈90 m).

Most bathymetric data coverage comes from National Ocean Service (NOS) surveys performed for nautical charting; NOS surveys, completed between 1903 and 2008, provide nearly complete coverage of the navigable parts of the survey area. Multibeam swath sonar and single-beam track line survey data provided additional coverage for limited areas, mostly in deep water. The US Army Corps of Engineers (USACE) provided recent survey results for the dredged Cordova harbor area, which it is responsible for maintaining. The Copper River Delta area changes frequently and lacks recent survey data; NGDC digitized estimated depth points for this area, and expects that the gridded depths in this area may be inaccurate (Grothe et al 2010). This region is well separated from the Cordova and can be expected to have little effect on tsunami wave dynamics at the town.

Topographic data in the NGDC source is from the US Geological Survey's National Elevation Dataset (USGS NED). This dataset provides nationwide coverage at 2-arc-seconds, but has a variable vertical accuracy of ± 7-15 m. Further, no surveying to determine the precise relationship between the NED's original geodetic vertical datum (NGVD 29) to the tidal datum (MHW) used by the model grids have been performed in the Cordova area. Without this geodetic survey, NGVD 29 is estimated to be equivalent to local mean sea level (Grothe et al 2010); this may not always be the case in a given local area. However, figure [profile-graph] shows three across-shore profiles that do not show a substantial step at the coastline, indicating that this datum estimate is fairly good given the information available..

In tsunami modeling, forecasts of inundation flow depths and extents are highly sensitive to the accuracy of the input topographic data (Tang *et al* 2009), so flooding forecasts for Cordova may have inaccuracies. Two types of survey would, if both completed, substantially improve the reliability of flooding forecasts in the Cordova area. First is a survey to determine the exact vertical relationship between tidal and geodetic datums. Second is collection of high-resolution topographic and near-shore bathymetric data using aircraft-based LIDAR.

Model setup

Model grids were developed by cropping and resampling the source grids. MOST version 2, the version of the numerical model currently in operational use, requires a series of three nested grids for inundation modeling. The outermost grid is designated the A grid, the middle grid the B grid, and the innermost and highest resolution grid the C grid (Fig. [grid-extents]).

For this model, the extent of the A grid was set to reach to at least 1000 m depth along its southern boundary, and to include the all of the entrances to Prince William Sound from the Gulf of Alaska. This outer grid is designed to capture wave dynamics as

far-field tsunami approaches the continental shelf. In shallower on-shelf waters, the non-linear components of the shallow-water equations become large, requiring a transition from the pre-computed propagation database to the inundation forecast model.

The B grid was designed to include the two narrow passages to Orca Bay and the Cordova area, from the northwest and the south. The high-resolution C grid covers the town of Cordova and the shoreline areas on both sides of its harbor that are expected to have the greatest impact on local wave dynamics.

Table [most-setup] contains details of the model grid and parameter setup. For the MOST model, grid nodes are georeferenced in spherical coordinates (decimal degrees). At Cordova's latitude, using a longitudinal grid spacing (in decimal degrees) of twice the latitude spacing results in grid cells that are very nearly square.

Model validation and testing

The model testing process is intended to ensure that the model meets two major requirements that make it usable as part of an operational forecast system:

1. The model must accurately predict the actual wave dynamics at the location.
2. The model must be numerically stable for all plausible event source scenarios.

To validate model accuracy, we compare model results with tide gauge records for available events. To validate numerical stability, we use a suite of large earthquake source scenarios, as well as a very small (no-wave) scenario.

Historical event validation

As discussed above, Cordova has a limited tsunami history due to its well-protected location. Despite the limited archive of tide gauge records available, we can still run models of major past events to illustrate the range of tsunami impacts previously encountered at the town. Table [historic-events] lists the historic events used for this illustration and for testing.

Tables [unimak1946] through [japan2011] show computed maximum amplitudes and timeseries at the tide gauge for the reference and forecast models. In general, the correspondence at the tide gauge between the forecast and inundation models is good for all events. Arrival times are nearly always consistent, and maximum amplitude correspondence is excellent, except that the forecast model sometimes under-predicts the maximum amplitudes of later waves.

For the 2010 Chile (Fig. [chile201]) and 2011 Japan (Fig. [japan2011]) events, tide gauge records are also included in the timeseries plots. As discussed above, recorded tsunami amplitudes at Cordova are small relative to the signal noise. The models slightly over-predict early wave amplitudes. For the Japan tsunami, the largest wave at Cordova came 7.5 hours after the first wave arrival (16 hours after the event); the models did not correctly predict this late wave. Still, it was well within the maximum amplitude predicted at Cordova overall.

Model stability testing

In order to be a part of a reliable forecast system, each forecast model must be numerically stable under a wide range of source scenarios. The MOST model typically becomes unstable in one of two ways; it either produces unrealistically large amplitudes ("blows up"), or it produces small high-frequency waves ("ringing"). To test the model stability, a suite of very large and very small hypothetical source scenarios are used.

The large sources are Mw 9.3 events located along all major subduction zones in the Pacific Ocean; the sources are compiled by linear combination of twenty 100km by 50km unit sources, with each assigned a seismic slip of 25 m. The results at the Cordova tide gauge are shown in Fig. [stability-all].

In addition to stability with extremely large waves, the model was also validated to produce correct results with very small input boundary condition waves. In this situation, the model is expected to also output little or no waves; a numerically unstable model might produce ringing or increasing amplitudes in this situation. The forecast model was tested in this "no-wave" case by using an equivalent of a M7.0 earthquake along the East Philippines subduction zone.

Acknowledgements

References

Caldwell, R. J., B.W. Eakins, and E. Lim. 2009. Digital Elevation Models of Prince William Sound, Alaska: Procedures, Data Sources and Analysis. NOAA National Geophysical Data Center.

Grothe, P.R., L.A. Taylor, B.W. Eakins, R.J. Caldwell, E. Lim, and D.Z. Friday. 2010. Digital Elevation Models of Cordova, Alaska: Procedures, Data Sources and Analysis. NOAA National Geophysical Data Center.

Sepez, J.A, B.D. Tilt, C. L. Package, H. M. Lazrus, and I. Vaccaro. 2005. Community Profiles for North Pacific Fisheries –Alaska. NOAA Technical Memorandum NMFS-AFSC-160.

Tang, L., V.V. Titov, and C.D. Chamberlin. 2009: Development, testing, and applications of site-specific tsunami inundation models for real-time forecasting. J. Geophys. Res., 114, C12025, doi: 10.1029/2009JC005476.

Wilson, B.W. and A. Tørum. 1972. Effects of the tsunamis: an engineering study. In: National Academy of Sciences, *The Great Alaska Earthquake of 1964: Oceanography and coastal engineering*, Washington, DC. p361-523.

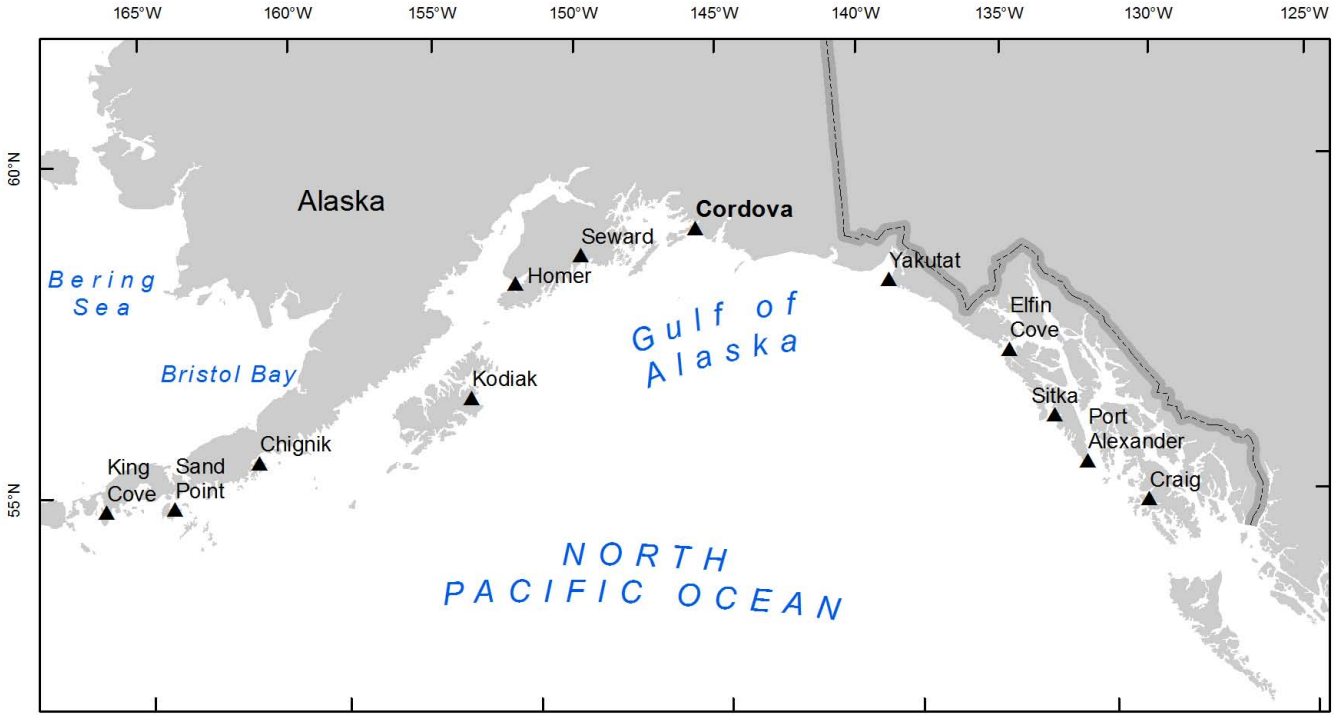
165°W
160°W
155°W
150°W
145°W
140°W
135°W
130°W
125°W
60°N
55°N
Alaska
Bering Sea
Bristol Bay
Gulf of Alaska
NORTH PACIFIC OCEAN
Cordova
Seward
Homer
Yakutat
Elfin Cove
Sitka
Port Alexander
Craig
Kodiak
Chignik
King Cove
Sand Point

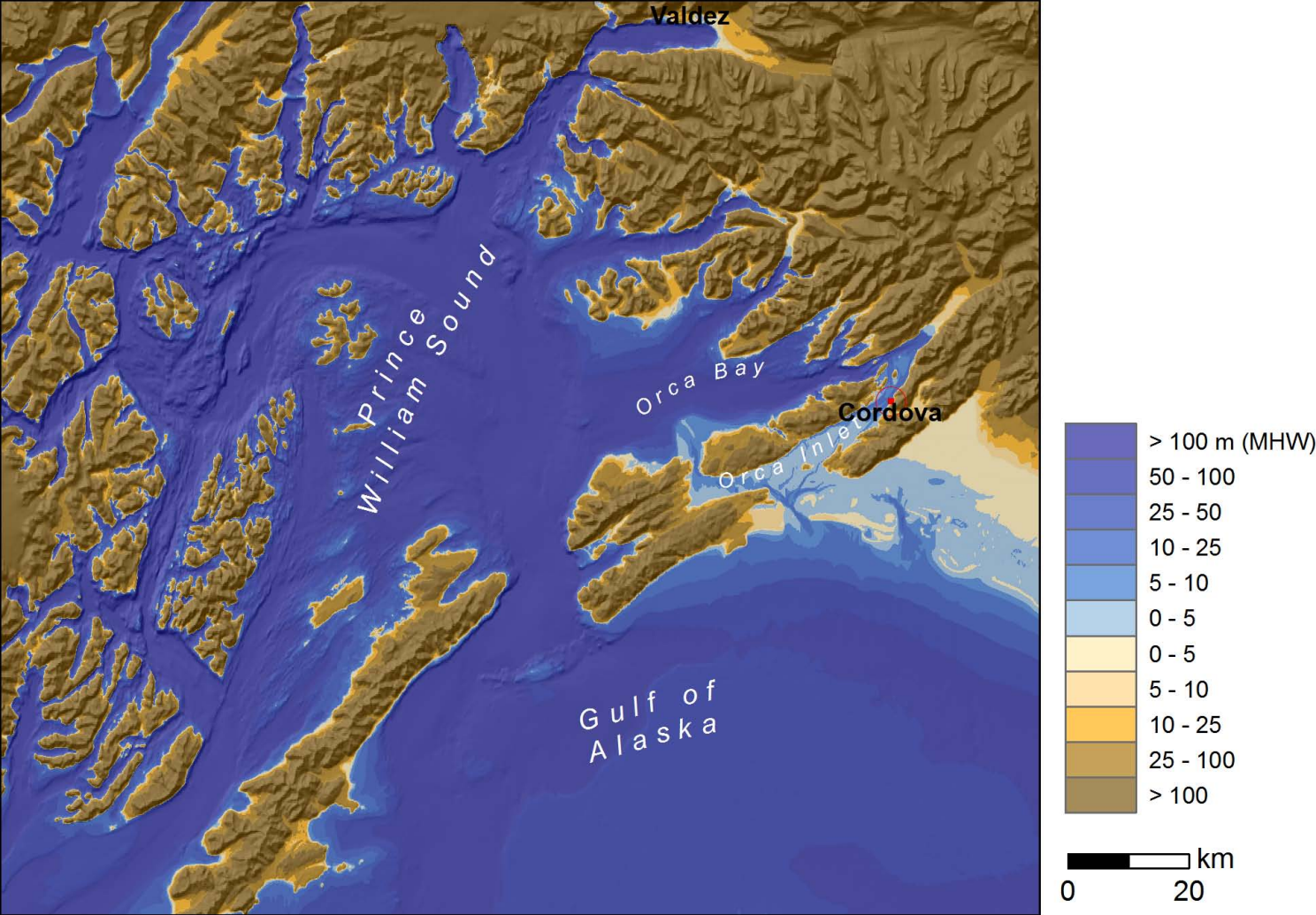
Valdez
Prince William Sound
Orca Bay
Orca Inlet
Cordova
Gulf of Alaska
> 100 m (MHW)
50 - 100
25 - 50
10 - 25
5 - 10
0 - 5
0 - 5
5 - 10
10 - 25
25 - 100
> 100
km
0
20

Below MLW
MLW - MHW
Above MHW

km
0 6

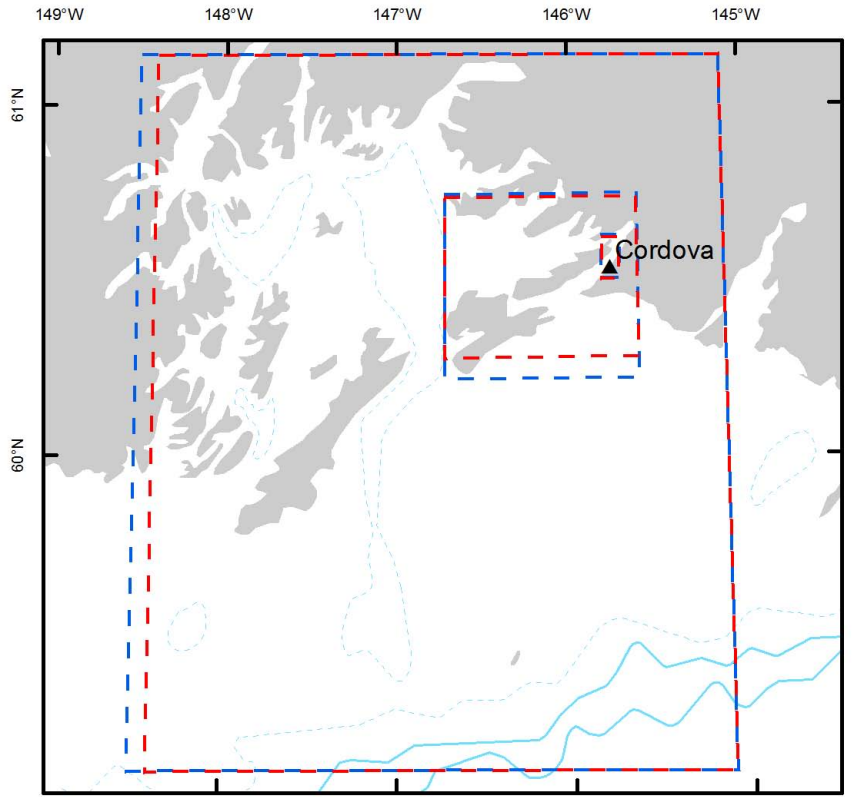
149°W
148°W
147°W
146°W
145°W
61°N
60°N
Cordova

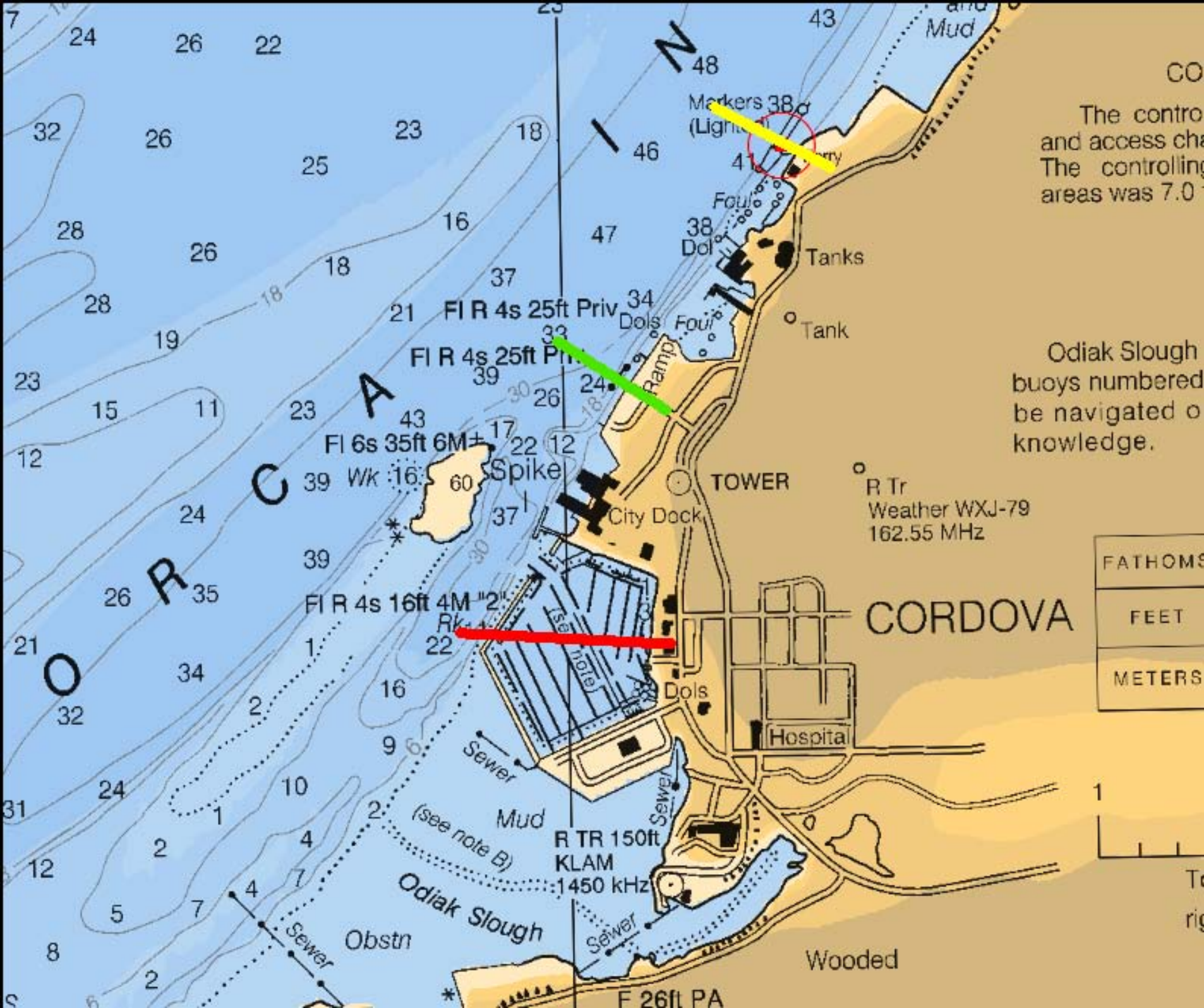
Markers 38d
(Light)
Fl R 4s 25ft Priv
Fl R 4s 25ft Priv
Fl 6s 35ft 6M±
Spike
Fl R 4s 16ft 4M "2"
R TR 150ft
KLAM
1450 kHz
Odiak Slough
Obstn
Wooded
F 26ft PA
TOWER
City Dock
CORDOVA
Hospital
Tanks
Tank
Ramp
Dols
Foul
Sewer
Mud
R Tr
Weather WXJ-79
162.55 MHz
Odiak Slough
buoys numbered
be navigated o
knowledge.
FATHOMS
FEET
METERS
(see note B)
(see note)

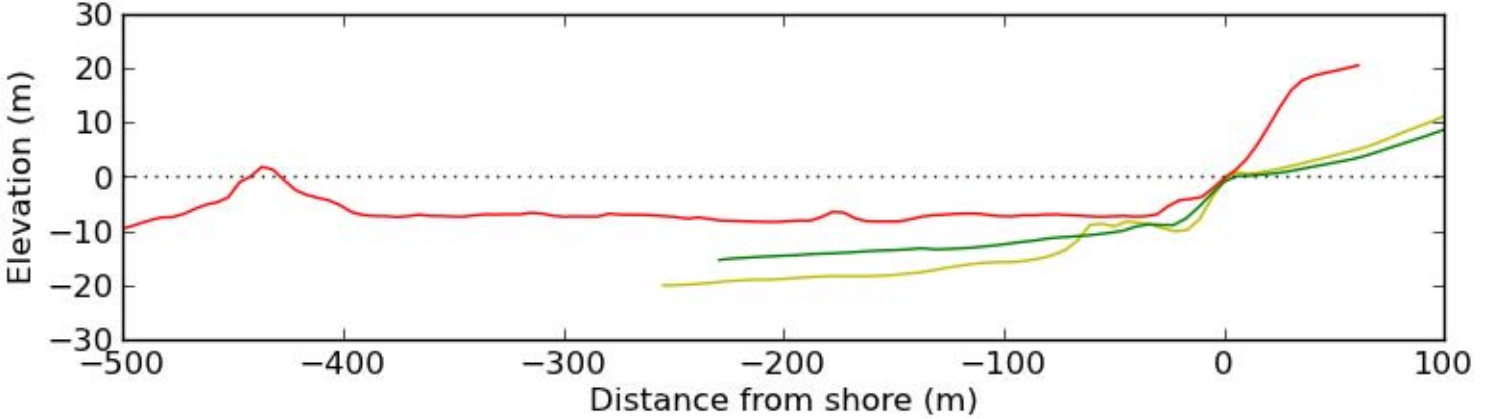
30
20
10
0
−10
−20
−30
Elevation (m)
−500
−400
−300
−200
−100
0
100
Distance from shore (m)

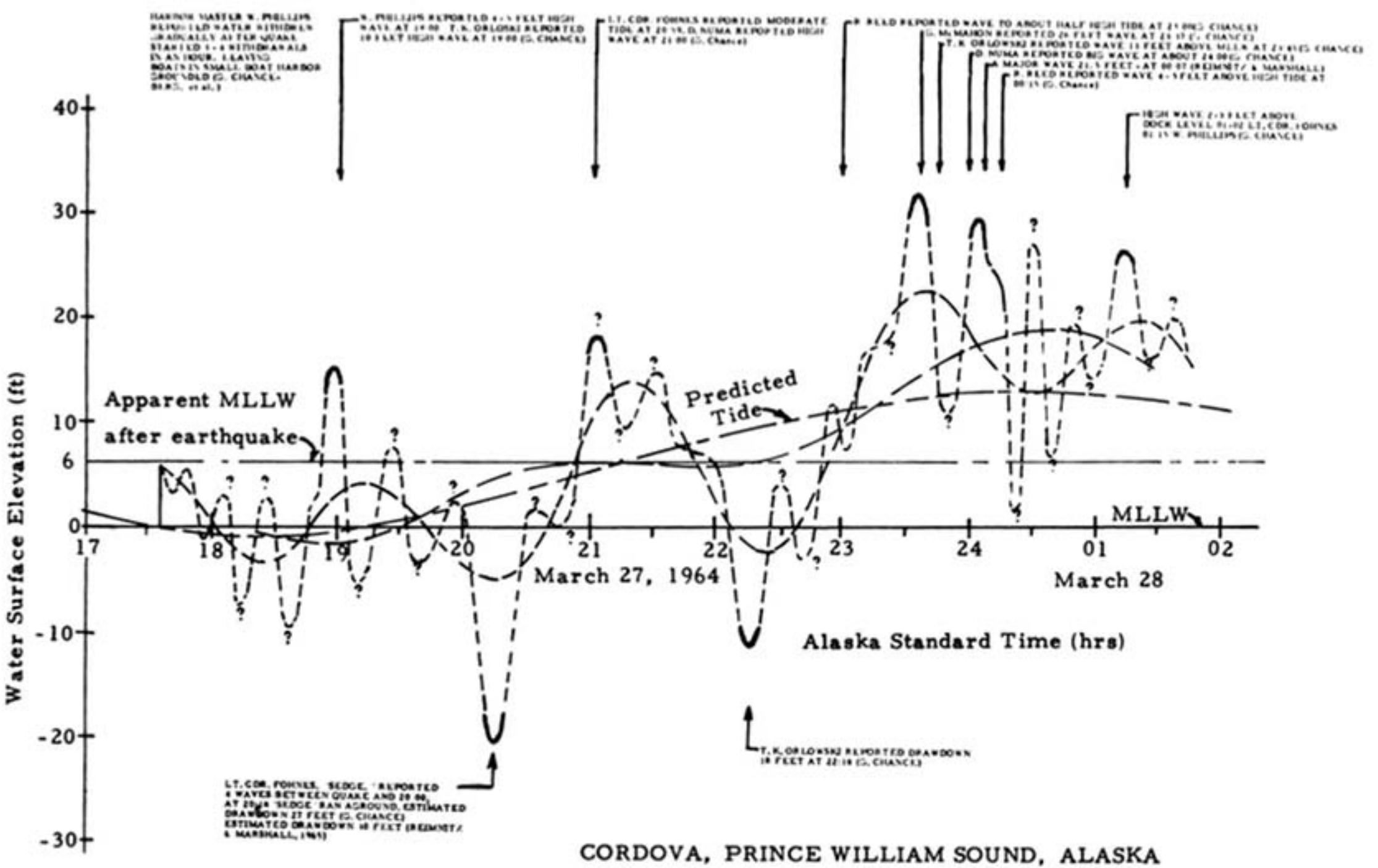

FIGURE 121 Inferred marigram for Cordova, based on accounts by eyewitnesses and on inductive reasoning.

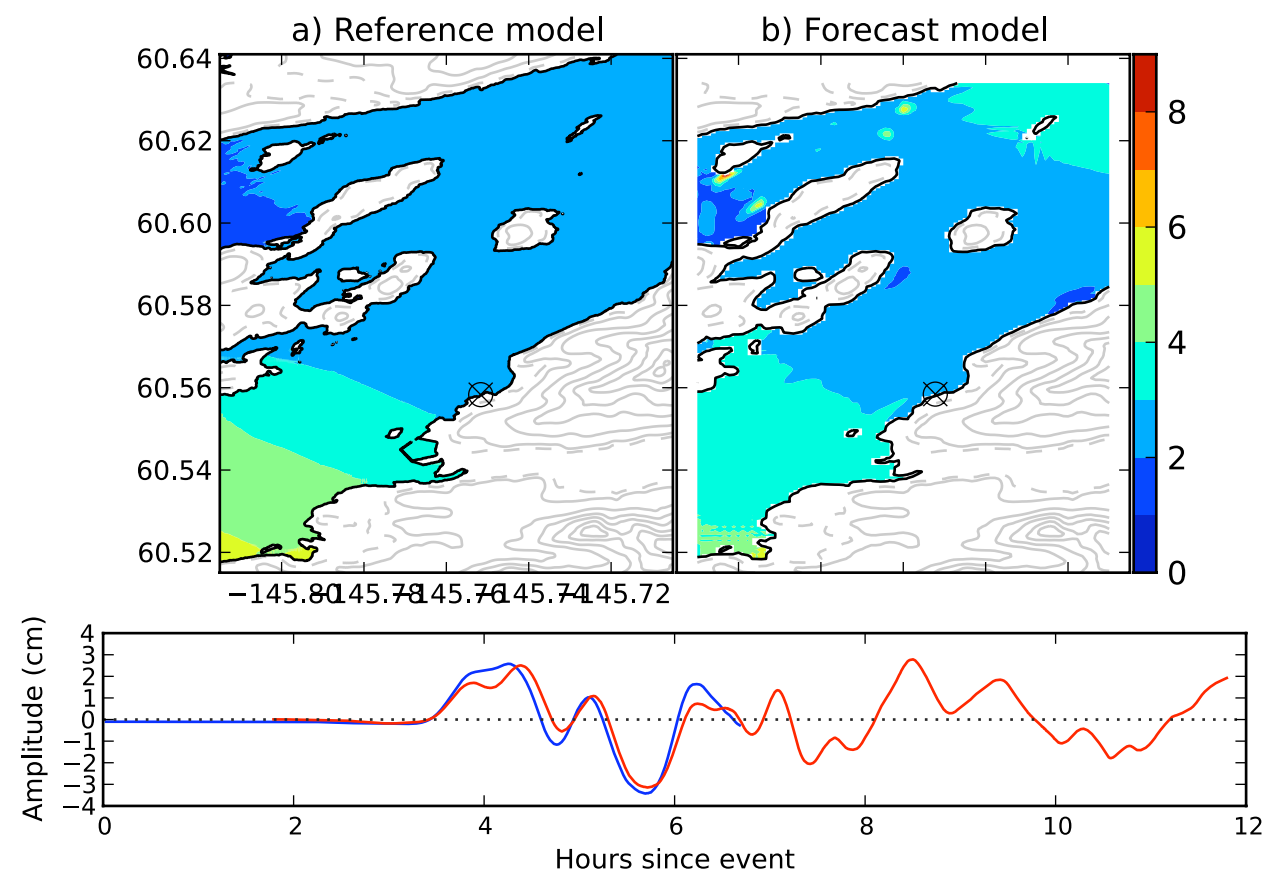
a) Reference model
b) Forecast model
60.64
60.62
60.60
60.58
60.56
60.54
60.52
−145.80
−145.78
−145.76
−145.74
−145.72
8
6
4
2
0
Amplitude (cm)
4
3
2
1
0
−1
−2
−3
−4
0
2
4
6
8
10
12
Hours since event

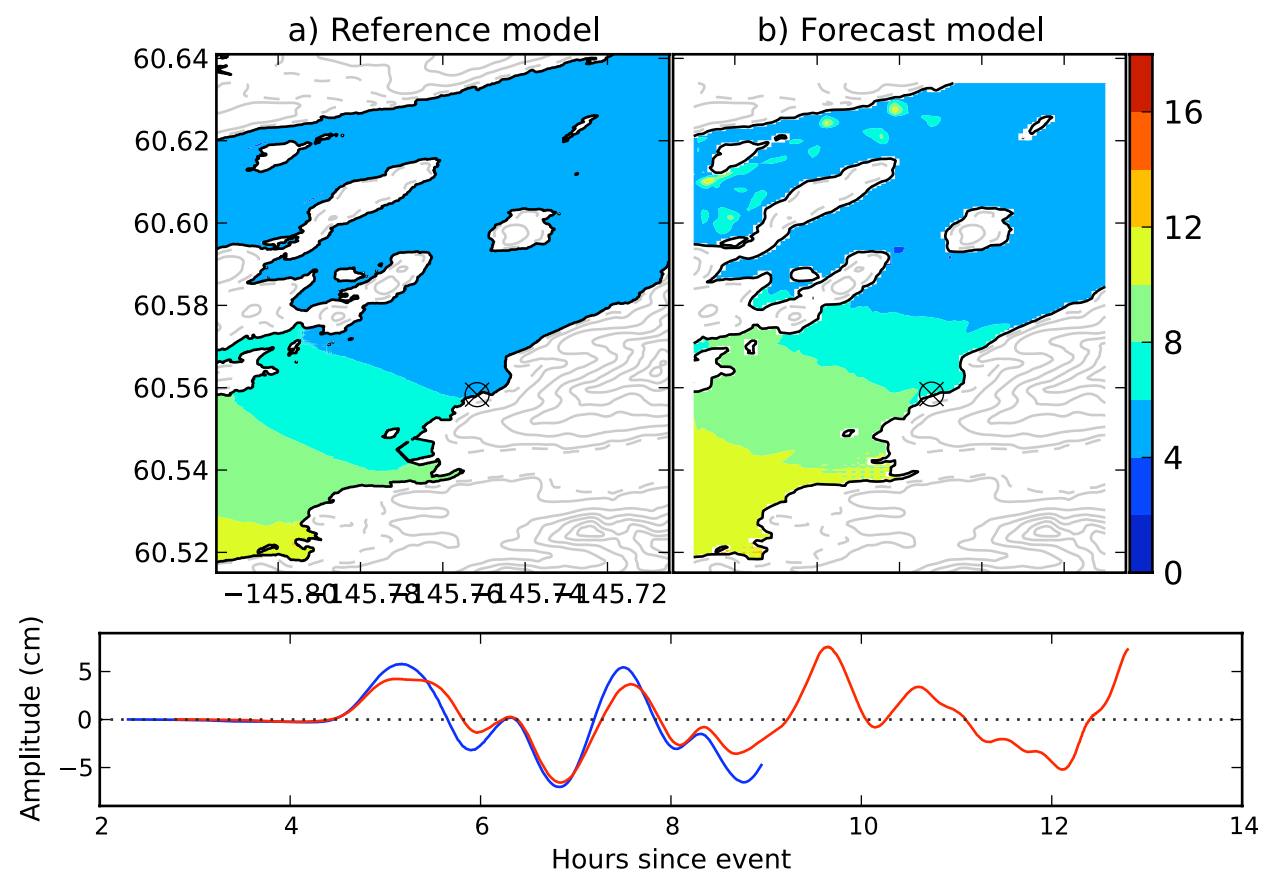
a) Reference model
b) Forecast model
60.64
60.62
60.60
60.58
60.56
60.54
60.52
−145.80
−145.78
−145.76
−145.74
−145.72
16
12
8
4
0
Amplitude (cm)
5
0
−5
2
4
6
8
10
12
14
Hours since event

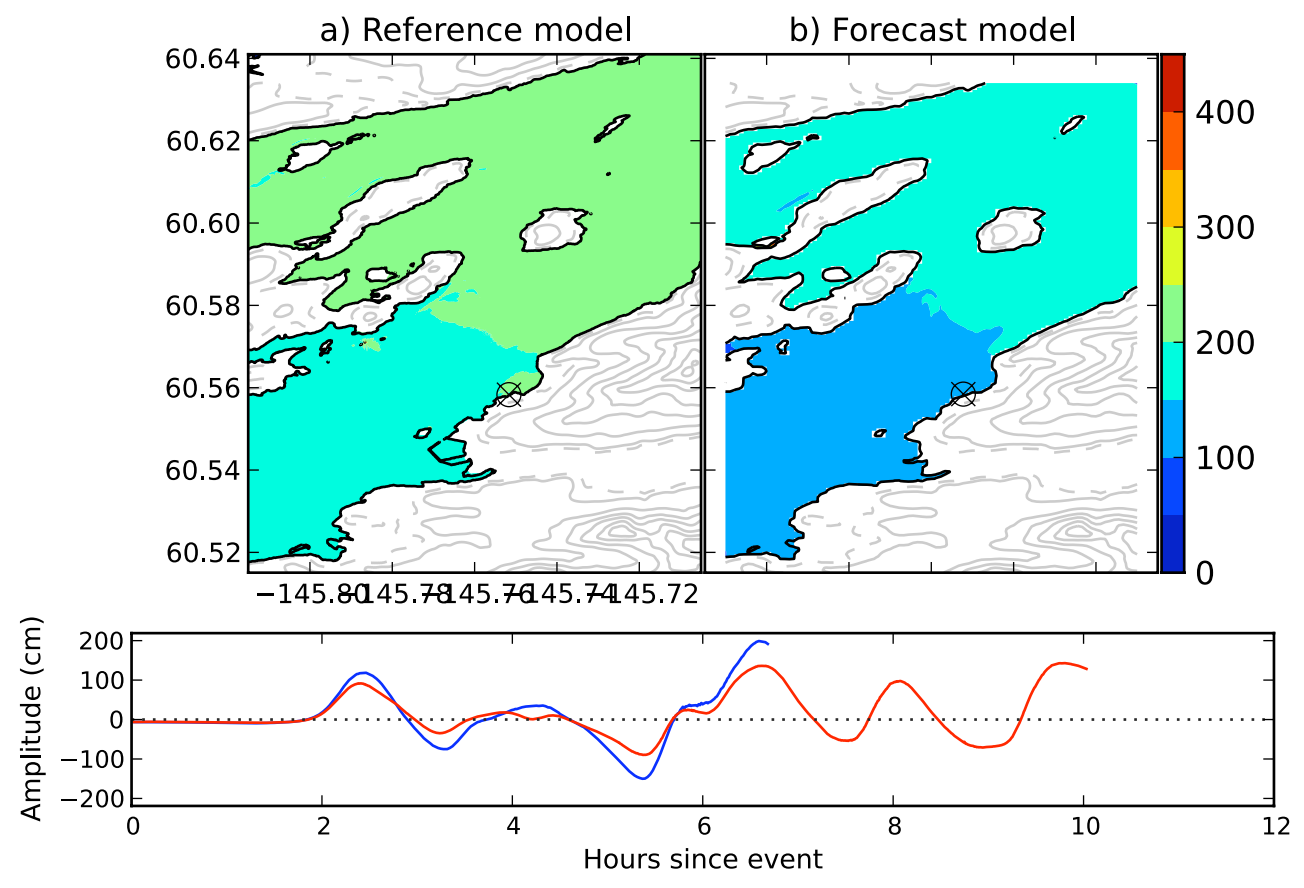
a) Reference model
b) Forecast model
60.64
60.62
60.60
60.58
60.56
60.54
60.52
−145.80
−145.78
−145.76
−145.74
−145.72
400
300
200
100
0
Amplitude (cm)
200
100
0
−100
−200
0
2
4
6
8
10
12
Hours since event

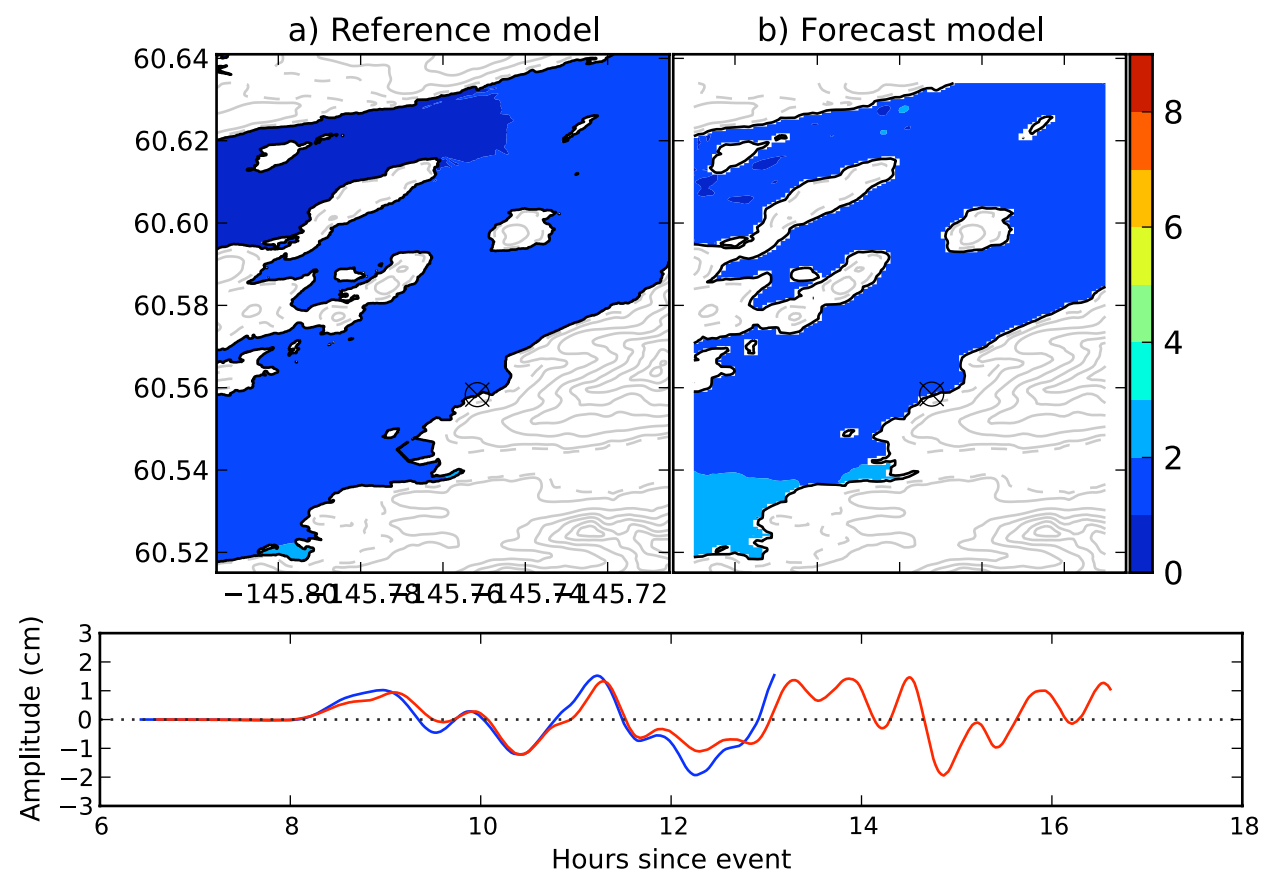
a) Reference model
b) Forecast model
60.64
60.62
60.60
60.58
60.56
60.54
60.52
−145.80
−145.78
−145.76
−145.74
−145.72
8
6
4
2
0
Amplitude (cm)
3
2
1
0
−1
−2
−3
6
8
10
12
14
16
18
Hours since event

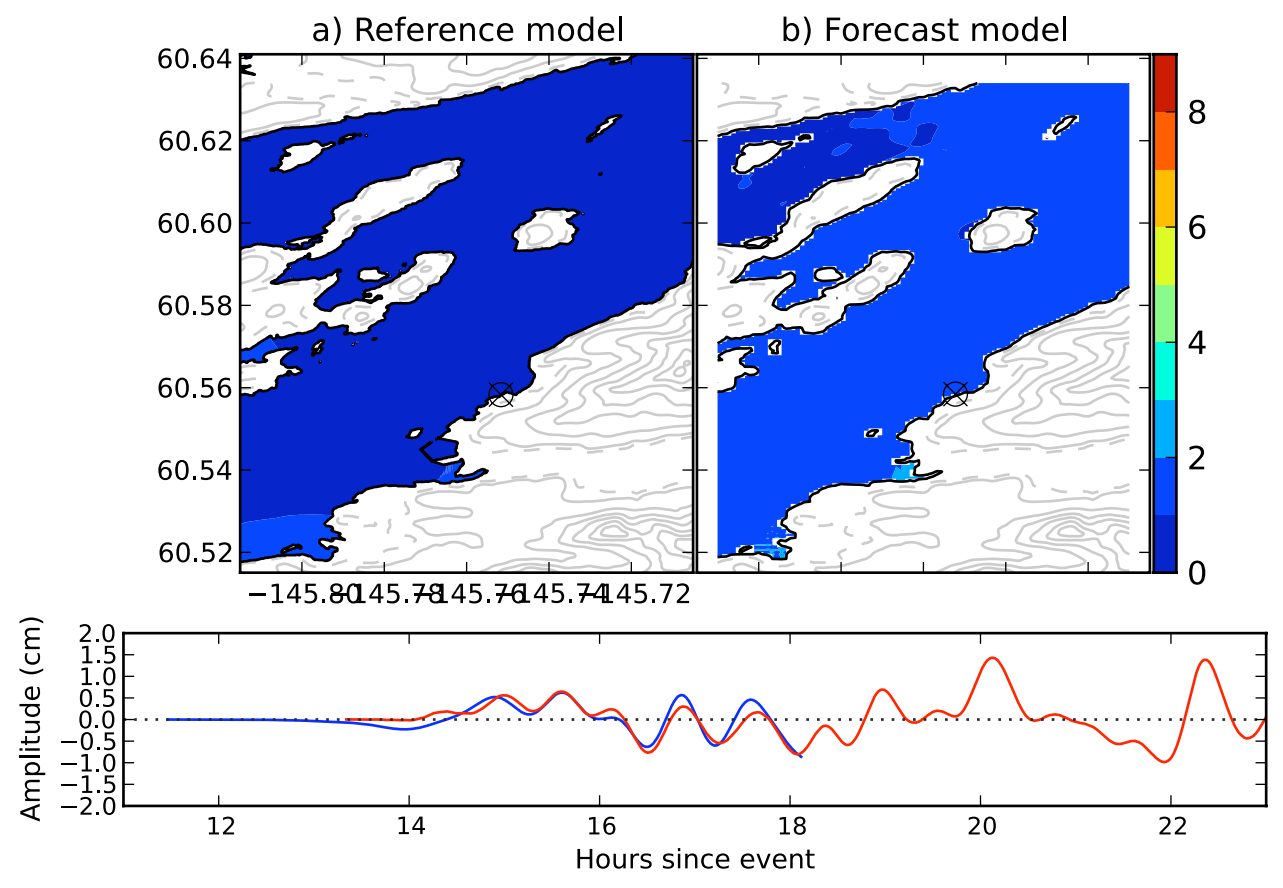
a) Reference model
b) Forecast model
60.64
60.62
60.60
60.58
60.56
60.54
60.52
−145.80
−145.78
−145.76
−145.74
−145.72
8
6
4
2
0
Amplitude (cm)
2.0
1.5
1.0
0.5
0.0
−0.5
−1.0
−1.5
−2.0
12
14
16
18
20
22
Hours since event

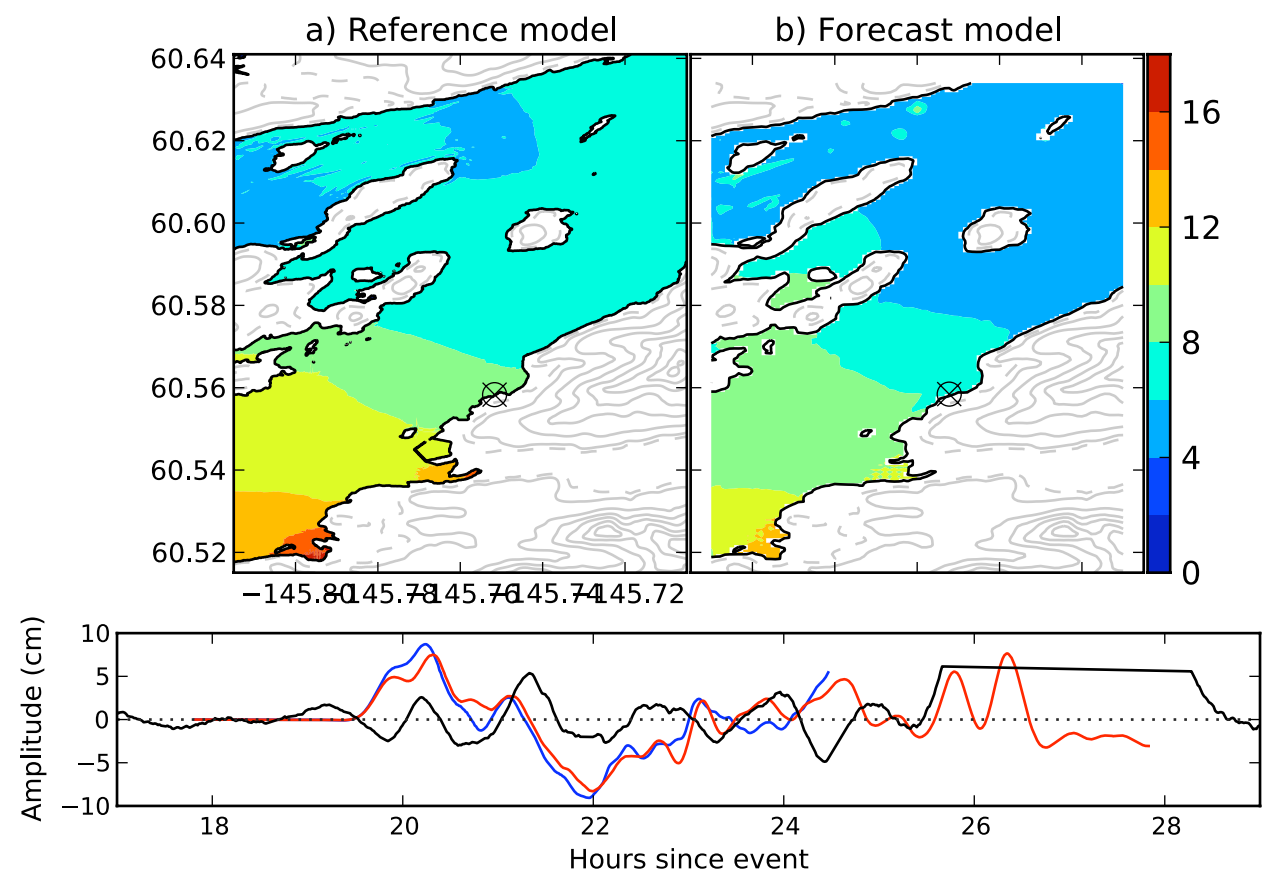
a) Reference model
b) Forecast model
60.64
60.62
60.60
60.58
60.56
60.54
60.52
−145.80
−145.78
−145.76
−145.74
−145.72
16
12
8
4
0
Amplitude (cm)
10
5
0
−5
−10
18
20
22
24
26
28
Hours since event

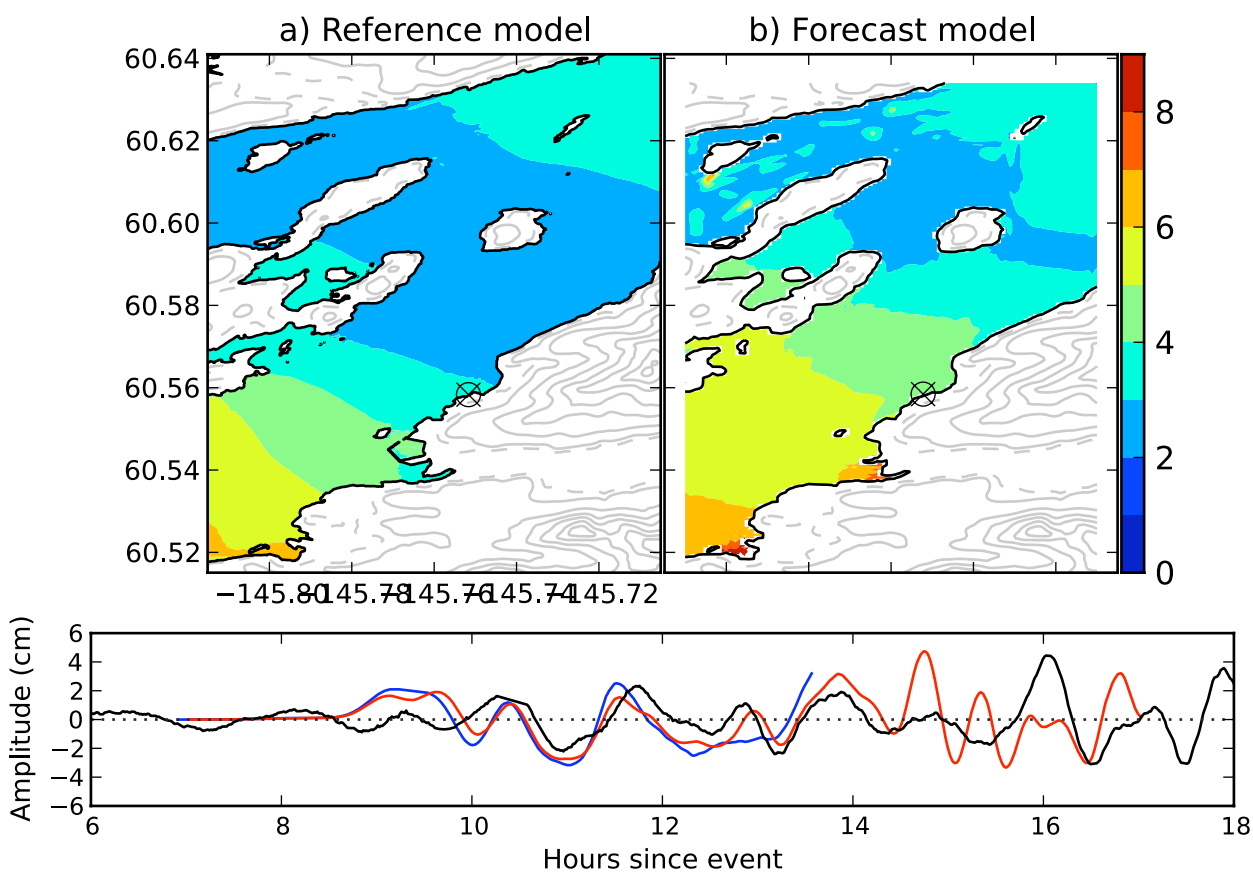
a) Reference model
b) Forecast model
60.64
60.62
60.60
60.58
60.56
60.54
60.52
−145.80
−145.78
−145.76
−145.74
−145.72
8
6
4
2
0
Amplitude (cm)
6
4
2
0
−2
−4
−6
6
8
10
12
14
16
18
Hours since event

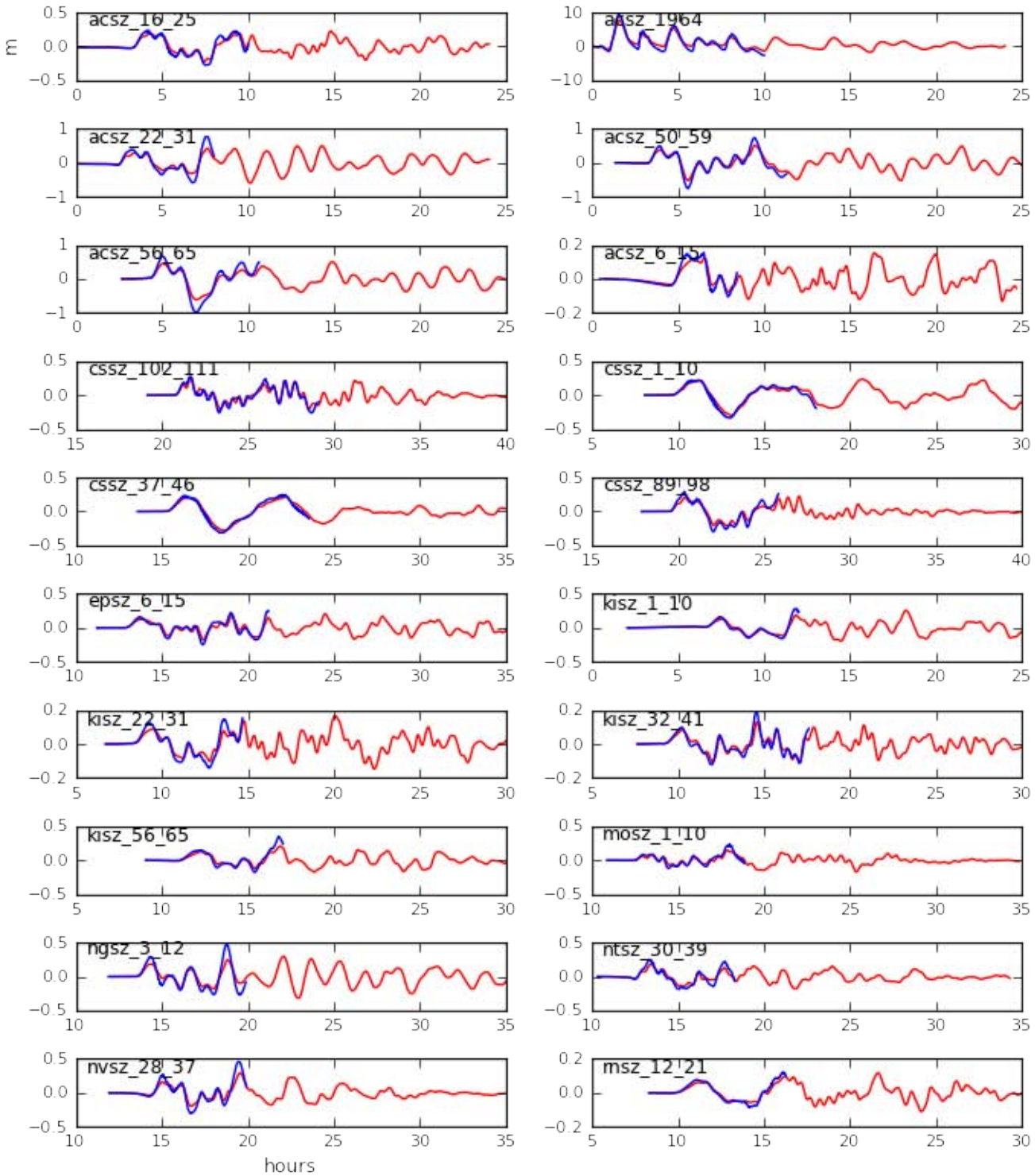
m
acsz_16_25
acsz_1964
acsz_22_31
acsz_50_59
acsz_56_65
acsz_6_15
cssz_102_111
cssz_1_10
cssz_37_46
cssz_89_98
epsz_6_15
kisz_1_10
kisz_22_31
kisz_32_41
kisz_56_65
mosz_1_10
ngsz_3_12
ntsz_30_39
nvsz_28_37
msz_12_21
hours